

Coherent pion production by neutrinos

Emmanuel A. Paschos*, Dario Schalla†

December 18, 2008

1 Introduction

This paper is supposed to summarize the content of my diploma thesis. It is based on the theory by Gounaris, Kartavtsev and Paschos [1]. It describes the reactions

$$\nu_\mu N \rightarrow \nu_\mu N \pi^0 \quad (1)$$

$$\nu_\mu N \rightarrow \mu^- N \pi^+ \quad (2)$$

where N is a heavy nucleus that remains completely intact and does not change quantum numbers during the process. The corresponding Feynman diagrams are shown in figure 1.

Due to the weak isospin properties of the charged and neutral current the charged one is twice as big as the neutral one. Further difference rise from the non vanishing mass of the outgoing lepton and the additional CKM-matrix-element in the charged current case. Altogether one can concentrate on the charged current and extract the neutral one from it by setting the lepton mass to zero and dividing by two.

2 Triply differential cross section

The invariant matrix element of charged current coherent pion production by neutrinos is given by

$$\mathcal{M} = -\frac{G_F V_{ud}}{\sqrt{2}} j_\mu J^\mu, \quad (3)$$

where G_F is the Fermi coupling constant and V_{ud} the CKM-matrix element.

The leptonic current can be expressed by

$$j_\mu = \bar{u}(k') \gamma_\mu (1 - \gamma_5) u(k) \quad (4)$$

whereas the hadronic current has to be written more general in terms of vector and axialvector currents:

$$J_\mu = \mathcal{V}_\mu^+ - \mathcal{A}_\mu^+ \quad (5)$$

*paschos@physik.uni-dortmund.de

†dario.schalla@tu-dortmund.de

with

$$\mathcal{V}_\mu^\dagger = \langle \pi^+ N | V_\mu^1 + iV_\mu^2 | N \rangle \quad \mathcal{A}_\mu^\dagger = \langle \pi^+ N | A_\mu^1 + iA_\mu^2 | N \rangle. \quad (6)$$

The leptonic current can be decomposed into the basis of polarisation vectors. Due to the non conservation of the leptonic current caused by the finite lepton mass there are both spin zero and spin one degrees of freedom.

The spin zero degree of freedom corresponds to the following polarisation vector that is collinear to the four momentum transfer $q_\mu = k_\mu - k'_\mu$:

$$\epsilon_\mu^l = \frac{q_\mu}{\sqrt{Q^2}} = \frac{1}{\sqrt{Q^2}} \begin{pmatrix} \nu \\ 0 \\ 0 \\ |\vec{q}| \end{pmatrix}. \quad (7)$$

The spin one degree of freedom consists of the following three polarisations:

$$\epsilon_\mu(\lambda = \pm 1) = \mp \frac{1}{\sqrt{2}} \begin{pmatrix} 0 \\ 1 \\ \pm i \\ 0 \end{pmatrix} \quad \epsilon_\mu(\lambda = 0) = \frac{1}{\sqrt{Q^2}} \begin{pmatrix} |\vec{q}| \\ 0 \\ 0 \\ \nu \end{pmatrix}. \quad (8)$$

They fulfill the completeness relation

$$\sum_{\lambda=0,\pm 1} (-1)^\lambda \epsilon^\mu(\lambda) \epsilon^{\nu*}(\lambda) - \epsilon_l^\mu \epsilon_l^\nu = g^{\mu\nu}. \quad (9)$$

By squaring the matrix element and averaging the spins the transition possibility can be written in terms of a leptonic and a hadronic tensor:

$$|\overline{\mathcal{M}}|^2 = \frac{G_F^2 |V_{ud}|^2}{2} T^{\mu\nu} H_{\mu\nu}. \quad (10)$$

Using the normalisation of the polarization vectors the leptonic tensor can be written in terms of density matrix elements:

$$\begin{aligned} |\overline{\mathcal{M}}|^2 &\propto T_{\mu\nu} H^{\mu\nu} \\ &= \sum_{i,j} \epsilon_{i\mu} \epsilon_i^{\mu*} T_{\mu\nu} J^\mu J^{\nu\dagger} \\ &= \sum_{i,j} \epsilon_{i\mu} L_{ij} \epsilon_{j\nu}^* J^\mu J^{\nu*} \\ &= \sum_{i,j} L_{ij} (\epsilon_{i\mu} J^\mu) (\epsilon_{j\nu} J^\nu). \end{aligned} \quad (11)$$

The couplings of scalar and longitudinal polarisations to left and right handed ($\lambda = \pm 1$) ones cancel out by averaging over the angle between the leptonic and the pion production plane [2].

Thus the squared matrix element can be written as:

$$|\overline{\mathcal{M}}|^2 = \frac{G_F^2 |V_{ud}|^2}{2} \left\{ L_{00} |J_\mu \epsilon_0^\mu|^2 + L_{ll} |J_\mu \epsilon_l^\mu|^2 + 2L_{l0} (J_\mu \epsilon_l^\mu) (J_\mu \epsilon_0^\mu)^* + L_{LL} |J_\mu \epsilon_L^\mu|^2 + L_{RR} |J_\mu \epsilon_R^\mu|^2 \right\}. \quad (12)$$

The density matrix elements turn out to be:

$$\begin{aligned}
L_{00} &= \frac{4[Q^2(2E_\nu - \nu) - \nu m_\mu^2]^2}{Q^2(Q^2 + \nu^2)} - 4(Q^2 + m_\mu^2) \\
L_{ll} &= \frac{4m_\mu^2[Q^2(2E_\nu - \nu) - \nu m_\mu^2]}{Q^2\sqrt{Q^2 + \nu^2}} \\
L_{l0} &= \frac{4m_\mu^2(Q^2 + m_\mu^2)}{Q^2}.
\end{aligned} \tag{13}$$

With

$$\tilde{L}_{ij} = \frac{1}{2}L_{ij}, \tag{14}$$

which rises from the non normalized polarisation vectors in [1], they are the same as given in [1].

The left and right handed matrix elements can be written as:

$$\frac{\tilde{L}_{LL} + \tilde{L}_{RR}}{2} = Q^2 \left[1 + \frac{(2E_\nu - \nu)^2}{Q^2 + \nu^2} \right] - \frac{m_\mu^2}{Q^2 + \nu^2} [2\nu(2E_\nu - \nu) + m_\mu^2]. \tag{15}$$

The next step is to calculate the couplings of the hadronic current to the polarisation vectors in equation (12). For that purpose the partially conserved axial vector current (PCAC) is used. This step leads to the creation of the pion.

The decay of a pion is defined by

$$\langle 0 | A_a^\mu | \pi_b \rangle = -if_\pi q^\mu e^{-iq \cdot x} \delta_{ab}, \tag{16}$$

where a and b indicate the conservation of the isovector. f_π is the pion decay constant and q^μ the momentum of the pion.

The conservation of the current can be tested by its divergence:

$$\begin{aligned}
\langle 0 | \partial^\mu A_\mu^+ | \pi^+ \rangle &= -f_\pi m_\pi^2 e^{-ip \cdot x} \\
&= -iq^\mu \langle 0 | A_\mu^+ | \pi^+ \rangle.
\end{aligned} \tag{17}$$

Because of the non vanishing but small pion mass the axial current is only partially conserved.

If the initial state is not vacuum but a hadronic system this leads to the Adler-ralation [3]:

$$\langle \beta | \partial^\mu A_\mu^+ | \alpha \rangle = -iq^\mu \langle \beta | A_\mu^+ | \alpha \rangle \propto \frac{m_\pi^2}{Q^2 + m_\pi^2} T(\alpha + \pi^+ \rightarrow \beta). \tag{18}$$

The term $T(\alpha + \pi^+ \rightarrow \beta)$ is the invariant amplitude of the indicated process.

Using these equations together with the above definition of the pion decay constant, one can make the following ansatz:

$$-i\mathcal{A}_\mu^+ = \frac{f_\pi \sqrt{2} q_\mu}{Q^2 + m_\pi^2} T(\pi^+ N \rightarrow \pi^+ N) - \mathcal{R}_\mu. \tag{19}$$

The quantity \mathcal{R}_μ includes contributions from other isovector axial mesons like $a_1(1260)$ that are considered to be a smooth function in Q^2 because they are quite far away from this region.

The scalar product of the axial current and the momentum transfer is

$$q_\mu \mathcal{R}^\mu = -f_\pi \sqrt{2} T(\pi^+ N \rightarrow \pi^+ N). \quad (20)$$

To calculate the products of the polarisation vectors and the hadronic current in equation (12) an approximation has to be made:

$$|\vec{q}|^2 \approx \nu^2 \Rightarrow \epsilon_\mu^0 \approx \frac{q_\mu}{\sqrt{Q^2}}. \quad (21)$$

To keep this approximation satisfied the parameter ξ is introduced. It is defined as

$$\nu = \xi \sqrt{Q^2} \quad (22)$$

so that the relation holds best for bigger ξ values.

Using this the first coupling is

$$\begin{aligned} J_\mu \epsilon_0^\mu &= (\mathcal{V}_\mu^+ - \mathcal{A}_\mu^+) \epsilon_0^\mu = -\mathcal{A}_\mu^+ \epsilon_0^\mu = -i \mathcal{R}_\mu \epsilon_0^\mu \\ &= -i \frac{f_\pi \sqrt{2}}{\sqrt{Q^2}} T(\pi^+ N \rightarrow \pi^+ N). \end{aligned} \quad (23)$$

The other is found to be

$$J_\mu \epsilon_l^\mu = -i \frac{f_\pi \sqrt{2}}{\sqrt{Q}} \frac{m_\pi^2}{Q^2 + m_\pi^2} T(\pi^+ N \rightarrow \pi^+ N). \quad (24)$$

The couplings of the hadronic current to the left and right handed polarisation vectors leads to scattering amplitudes of pion photoproduction $\gamma N \rightarrow \pi^0 N$ and transverse axial production of pions $A_T^+ N \rightarrow \pi^+ N$. Both of them can be estimated and compared to the contributions of the pion nucleus elastic scattering cross section. It is found that the latter one dominates the others and that they are negligible.

Thus, considering flux and phase space of the process, one obtains the following triply differential cross section of charged current coherent pion production by neutrinos scattering off nuclei:

$$\frac{d\sigma_{CC}}{dQ^2 d\nu dt} = \frac{G_F^2 |V_{ud}|^2}{2(2\pi)^2} \frac{\nu}{E_\nu^2} \frac{f_\pi^2}{Q^2} \left\{ \tilde{L}_{00} + \tilde{L}_{ll} \left(\frac{m_\pi^2}{Q^2 + m_\pi^2} \right)^2 + 2\tilde{L}_{l0} \frac{m_\pi^2}{Q^2 + m_\pi^2} \right\} \frac{d\sigma_\pi}{dt}, \quad (25)$$

where σ_π denotes the elastic pion nucleus scattering cross section. The corresponding neutral current cross section is:

$$\frac{d\sigma_{NC}}{dQ^2 d\nu dt} = \frac{G_F^2 |V_{ud}|^2}{4(2\pi)^2} \frac{\nu}{E_\nu^2} \frac{f_\pi^2}{Q^2} \tilde{L}_{00} \frac{d\sigma_\pi}{dt}. \quad (26)$$

The coefficients of the hadronic cross section $d\sigma_\pi/dt$ is shown in figure 2. The lepton mass suppresses the differential cross section for low momentum transfers.

3 Integrated cross section

To integrate the differential cross sections the hadronic cross section $d\sigma_\pi/dt$ has to be defined first. For that purpose experimental data is used [4, 5]. At various pion energies they give the cross section in dependence of the laboratory angle which leads to the needed differential form. The data is fitted with the exponential model

$$\frac{d\sigma_\pi}{d|t|} = a \cdot e^{-b|t|} \quad (27)$$

which is indicated by scattering theory. The hadronic cross section is shown in figure 3.

With that input data the triply differential cross section is completely determined. It is shown in figure 4. Due to the definition of ξ the lower integration limit of ν is changed to

$$\max\left(\xi\sqrt{Q^2}, \nu_{min}\right) \leq \nu \leq \nu_{max}, \quad (28)$$

where ν_{min} and ν_{max} indicate the kinematically allowed limit.

In the figure you can see that the choice of $\xi = 1$ is almost like ν_{min} because the important region is already completely included. This means that the integrated cross section will be very similar.

By integrating the differential cross section over ν you get the simple differential cross section. As you can see in figure 5 the charged current cross section turns downwards at small Q^2 values due to its smaller phase space whereas the neutral current cross section reaches a finite value at $Q^2 = 0$.

That so-called Adler-point can be estimated as

$$\left. \frac{d\sigma_{NC}}{dQ^2} \right|_{Q^2=0} = \frac{G_F^2 f_\pi^2}{2\pi^2} \sigma_\pi \left\{ \ln \frac{E_\nu}{m_\pi} + \frac{m_\pi}{E_\nu} - 1 \right\} \Big|_{E_\nu \approx 1 \text{ GeV}} \approx 135 \cdot 10^{-40} \frac{\text{cm}^2}{\text{GeV}^2}, \quad (29)$$

where σ_π is the approximate total elastic cross section at the given neutrino energy.

The ν integrated cross section for several ξ values is shown in figure 6. It gives emphasis to the fact that $\xi = 0$ is almost identical to $\xi = 1$. Both charged and neutral current cross sections are the same for very small Q^2 values due to the definition in equation (28). For bigger ξ values higher Q^2 values gain more importance. The higher Q^2 region is not negligible at higher neutrino energies as you can see in figure 7. The cut-off at $Q^2 = 0.2 \text{ GeV}^2$ as it is introduced in the original paper [1] has to be expanded. It is not possible to choose the simple kinematic maximum because it quickly raises to non physical values. At high momentum transfers the target nucleus breaks up and the process is no longer coherent. The only way to define a Q^2 cut-off is indicated by experimental analysis. The identification of events in a scattering experiment is performed by kinematic characteristics of all possible reaction channels. In [6] all events with momentum transfers bigger than 4 GeV^2 are interpreted as incoherent background. Therefore this cut is also used within the Q^2 integration of the differential cross section:

$$Q_{min}^2 \leq Q^2 \leq \min(Q_{max}^2, 4 \text{ GeV}^2). \quad (30)$$

The integrated cross sections for different Q^2 cuts are shown in figures 8 and 9 for $\xi = 0$. This choice of the ξ parameter has been made to provide a

result that is comparable to experimental data. It is only a parameter within the theory that is not part of experimental analysis. Bigger values provide a good lower bound for the cross section whereas setting it to zero leads to some kind of expectation value for it.

The experimental data is given by [7, 8, 9, 10, 11]. Because the neutrino energy is widely spread, the position of the data point only indicates the mean value and is quite uncertain. Furthermore some experiments use a different target material than carbon as it is used within this theory. An analysis [12] of the dependence on the nuclear mass A of the target shows an approximate $A^{2/3}$ behaviour which is used to rescale the cross section values in the plot. This is the second uncertainty because this rough A -dependence has not been studied at higher energies so far. The theory is in good agreement with the experiments.

Especially the K2K measurement that provides a upper bound of charged current coherent pion production can be explained due to the inclusion of the lepton mass. A comparison between the correct and the zero lepton mass charged current cross section is shown in figure 10.

The neutral current cross section can be analytically approximated for high neutrino energies:

$$\sigma_{NC}(E_\nu) \approx \sigma_{NC}(E_\nu = \alpha) + \frac{2G_F^2 f_\pi^2 a}{\pi^2 b} \ln\left(\frac{E_\nu}{\alpha}\right) \text{ GeV}^2. \quad (31)$$

The bigger the expansion point α is the better the approximation holds. a and b are the parameters of the model given in equation (27) and are constant for big energies. A plot of the high energy region and the approximation together with some experimental data [13, 6, 14] is given in figure 11. They are also in good agreement.

4 Conclusion

The neutrino induced coherent pion production within the Gounaris-Kartavtsev-Paschos model provides a theoretical description that is based on PCAC. A strictly straight forward calculation of the Feynman diagram led to products of polarisation vectors and the hadronic current. Here the only approximation had to be made by assuming equation (21). Incorporating the mass of the outgoing lepton the integrated cross section is in good agreement with experimental data in both the neutral and the charged current case. Further investigation should include a deeper look at the Q^2 -cut-off because this is the most sensitive remaining parameter of the theory. An analysis of the dependence on the nuclear target would be useful, too, for a better comparison.

References

- [1] E. A. Paschos, A. Kartavtsev, and G. J. Gounaris, Phys. Rev. **D74**, 054007 (2006), hep-ph/0512139.
- [2] J. D. Bjorken and E. A. Paschos, Phys. Rev. **D1**, 3151 (1970).
- [3] S. L. Adler, Phys. Rev. **135**, B963 (1964).
- [4] CERN-IPN(Orsay), F. G. Binon *et al.*, Nucl. Phys. **B17**, 168 (1970).
- [5] T. Takahashi *et al.*, Phys. Rev. **C51**, 2542 (1995).
- [6] BEBC WA59, P. Marage *et al.*, Z. Phys. **C31**, 191 (1986).
- [7] J. L. Raaf, *A measurement of the neutrino neutral current pi0 cross section at MiniBooNE*, PhD thesis, University of Cincinnati, 2005, FERMILAB-THESIS-2005-20.
- [8] H. Faissner *et al.*, Phys. Lett. **B125**, 230 (1983).
- [9] E. Isiksal, D. Rein, and J. G. Morfin, Phys. Rev. Lett. **52**, 1096 (1984).
- [10] SKAT, H. J. Grabosch *et al.*, Zeit. Phys. **C31**, 203 (1986).
- [11] K2K, M. Hasegawa *et al.*, Phys. Rev. Lett. **95**, 252301 (2005), hep-ex/0506008.
- [12] D. Ashery *et al.*, Phys. Rev. C **23**, 2173 (1981).
- [13] CHARM-II, P. Vilain *et al.*, Phys. Lett. **B313**, 267 (1993).
- [14] E632, S. Willocq *et al.*, Phys. Rev. **D47**, 2661 (1993).

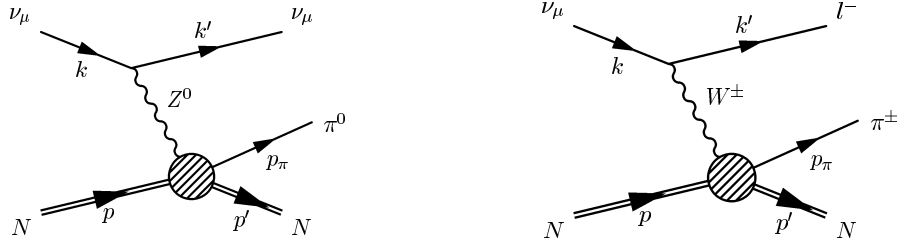


Figure 1: Feynman diagrams of neutral (left) and charged (right) current coherent pion production.

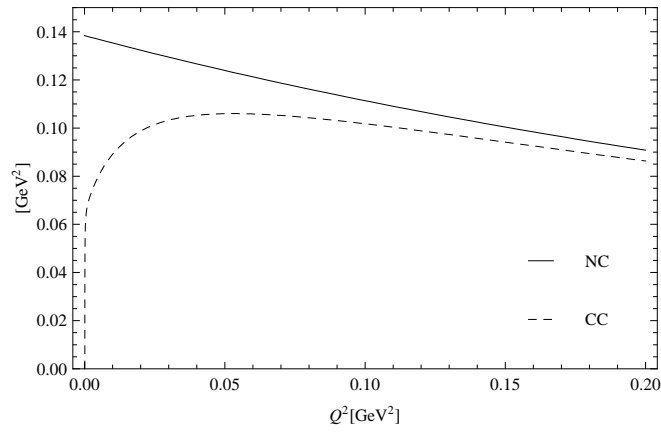


Figure 2: Coefficients of the hadronic cross section for $E_\nu = 2 \text{ GeV}$ and $\nu = 1 \text{ GeV}$.

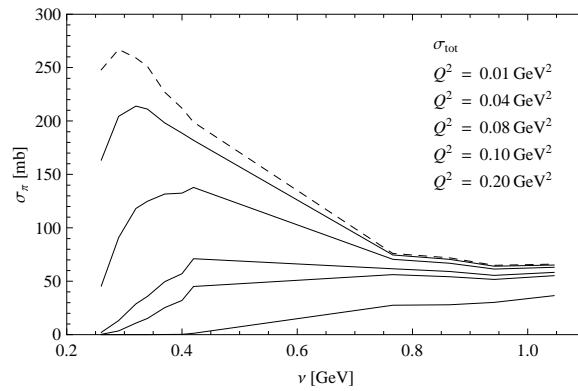


Figure 3: Hadronic cross section. The order of the curves is indicated in the plot.

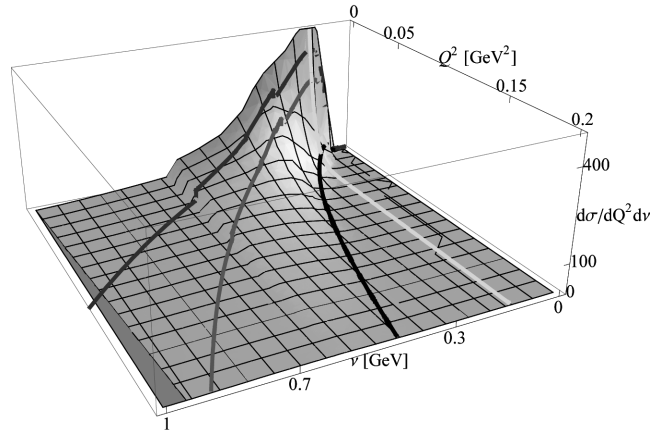


Figure 4: Neutral current differential cross section at $E_\nu = 1$ GeV. The lines show $\xi = 3, 2, 1$ and ν_{min} (from left to right).

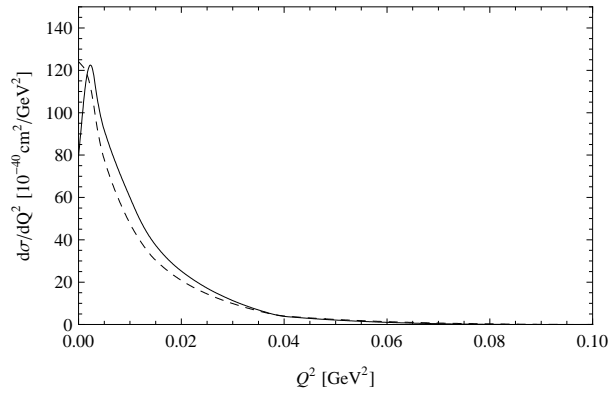


Figure 5: Simple differential cross section at $E_\nu = 1$ GeV for $\xi = 3$ in the neutral (dashed) and charged (straight) current case.

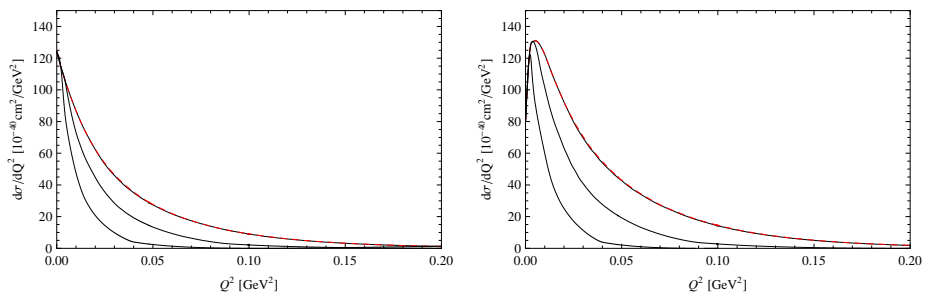


Figure 6: Differential cross section at $E_\nu = 1$ GeV for neutral (left) and charged (right) current for $\xi = 3, 2, 1$ (bottom to top) and $\xi = 0$ (dashed red).

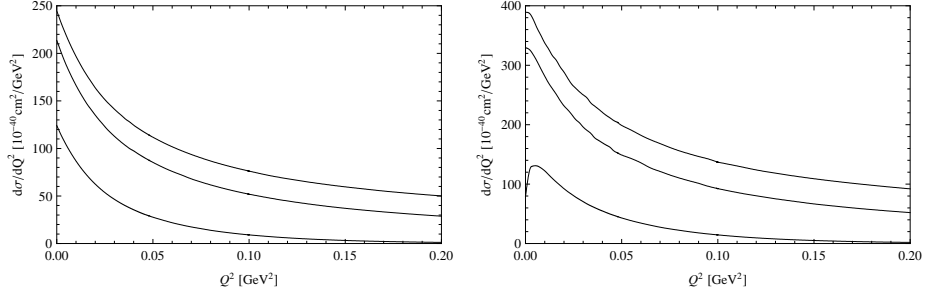


Figure 7: Differential cross section at $E_\nu = 1, 5$ and 10 GeV (bottom to top) with neutral (left) and charged (right) current for $\xi = 0$.

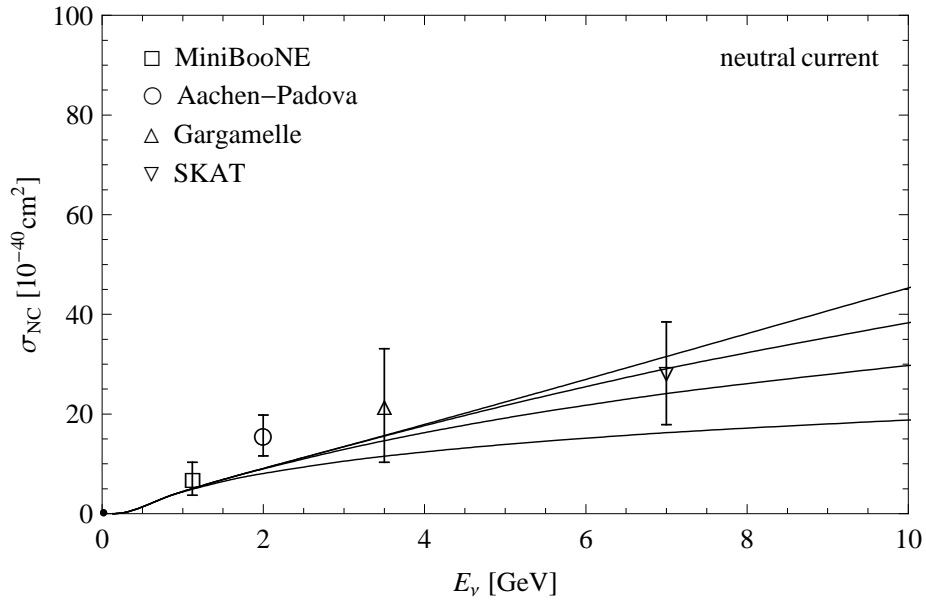


Figure 8: Integrated cross section for the neutral current process with $Q_{max}^2 = 0, 2$ GeV 2 , $Q_{max}^2 = 0, 5$ GeV 2 , $Q_{max}^2 = 1, 0$ GeV 2 und $Q_{max}^2 = 4, 0$ GeV 2 (bottom to top) for $\xi = 0$.

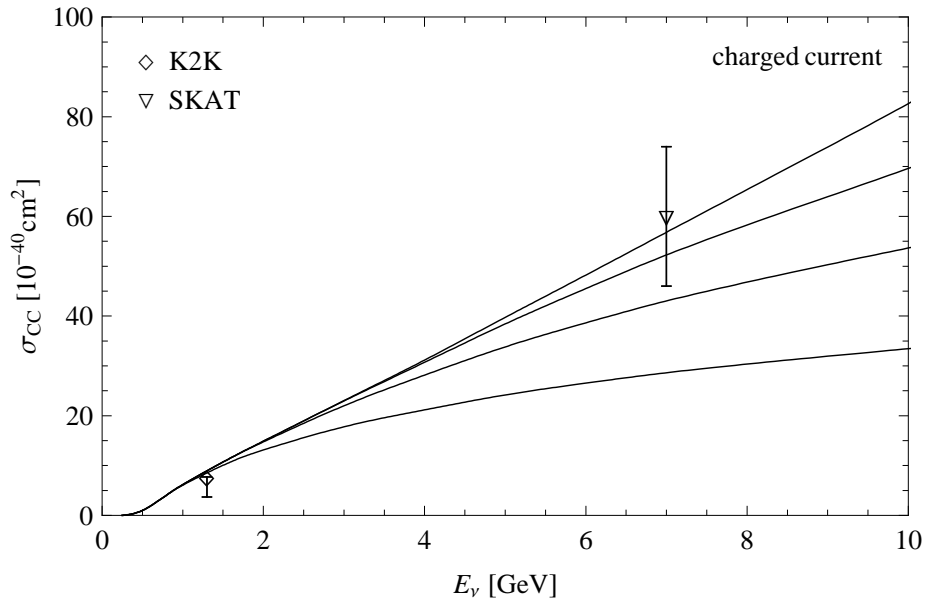


Figure 9: Integrated cross section for the charged current process with $Q_{max}^2 = 0,2 \text{ GeV}^2$, $Q_{max}^2 = 0,5 \text{ GeV}^2$, $Q_{max}^2 = 1,0 \text{ GeV}^2$ und $Q_{max}^2 = 4,0 \text{ GeV}^2$ (bottom to top) for $\xi = 0$.

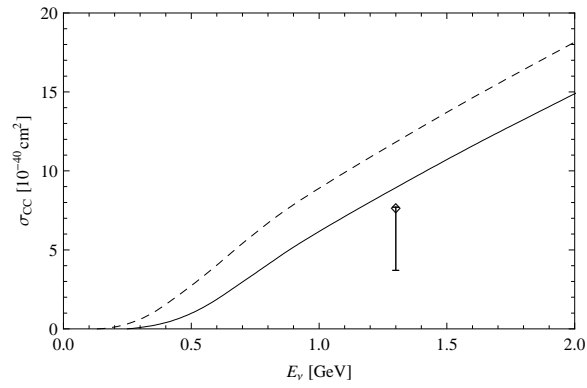


Figure 10: Charged current cross section with zero lepton mass (dashed) and correct lepton mass (straight) and K2K measurement [11].

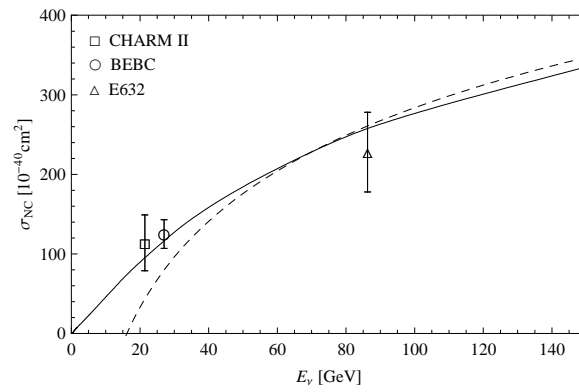


Figure 11: High energy neutral current cross section (straight) and approximation at $E_\nu = 70$ GeV (dashed).